Hindawi
Wireless Communications and Mobile Computing
Volume 2022, Article ID 2257338, 19 pages
https://doi.org/10.1155/2022/2257338

Research Article

Application Layer-Forward Error Correction Raptor Q Codes in 5G Mobile Networks for Factory of the Future

Athirah Mohd Ramly,[1] **Rosdiadee Nordin**,[2] **and Nor Fadzilah Abdullah**[2]

[1]*Department of Computing and Information System, School of Engineering and Technology, Sunway University, 47500 Subang Jaya, Selangor, Malaysia*
[2]*Department of Electrical, Electronics and System Engineering, Faculty of Engineering & Built Environment, Universiti Kebangsaan Malaysia, 43600 Bangi, Selangor, Malaysia*

Correspondence should be addressed to Rosdiadee Nordin; adee@ukm.edu.my

Received 22 December 2021; Revised 11 March 2022; Accepted 26 March 2022; Published 26 April 2022

Academic Editor: Chi-Hua Chen

The future communication requirements for industrial automation will differ significantly from existing technologies. Traffic in Industry 4.0 imposes real-time requirements, requiring ultra-reliable communication (URC) with high reliability and minimal latency. The demand for ultra-high reliability as high as 99.999999 percent and as low as 1 ms end-to-end latency is the major challenge of the NOMA communication system in the factory of the future. The high expectations on reliability and latency need modifications to the radio system's baseband signal processing, medium access control (MAC) layer, and application layer to protect against packet losses. Thus, this paper investigates the utilization of Raptor Q codes, which is a type of Application Layer Forward Error Correction (AL-FEC), by developing an end-to-end system level simulator to evaluate and analyze the performance of the transmission signals based on cross-layer approach; from the physical layer (PHY), MAC layer, and application layer parameters in an indoor factory network setting. The factory is assumed to be operated with various factory robots of different speeds, from static to 10 km/h. The 5G technology relies heavily on flexible network operations. High user density, high user mobility, deployment, and coverage are all qualities that allow for this flexibility. Through extensive simulations, the results showed that the Raptor Q codes are not only able to give good results, i.e., packet reception rate (PRR) = 0.9 of 10 m or 1.8% to 10 m or 3.4% depending on different scenarios, but are also able to meet PRR = 0.9 in the mobility scenario at 10 km/h. Thus, the Raptor Q codes can be seen as a good candidate for obtaining results within a strict range of requirements set by URC communications for the factory of the future replacing RLNC.

1. Introduction

Machine-to-machine (M2M) communication is a fundamental technology for the next-generation (5G) networks, allowing billions of multifunctional devices to interact with one another with little or no human involvement [1]. Furthermore, data packets are expected to include crucial information in several practical and promising 5G applications, such as autonomous driving and public safety systems, and should be sent with ultra-reliability and low latency [2]. The biggest issue with ultra-reliable and low-latency communication (URLLC) is to come up with a coding scheme that can handle ultra-reliable transmission [3]. In the recent decade, researchers have been particularly interested in rateless fountain codes. The first practical implementation of fountain codes was Luby transform (LT) codes [4]. With an average decoding cost of $O(k \log(k))$ operations, it can retrieve the original k information symbols. Researchers in [5] suggested Raptor codes, which combine an LT code with a high code rate precode to reduce decoding complexity further and solve the high error floor in LT codes. Furthermore, the 3rd Generation Partnership Project (3GPP) has already standardized a well-designed systematic Raptor code dubbed R10 code [6] composed of a systematic low-density generator matrix (LDGM)

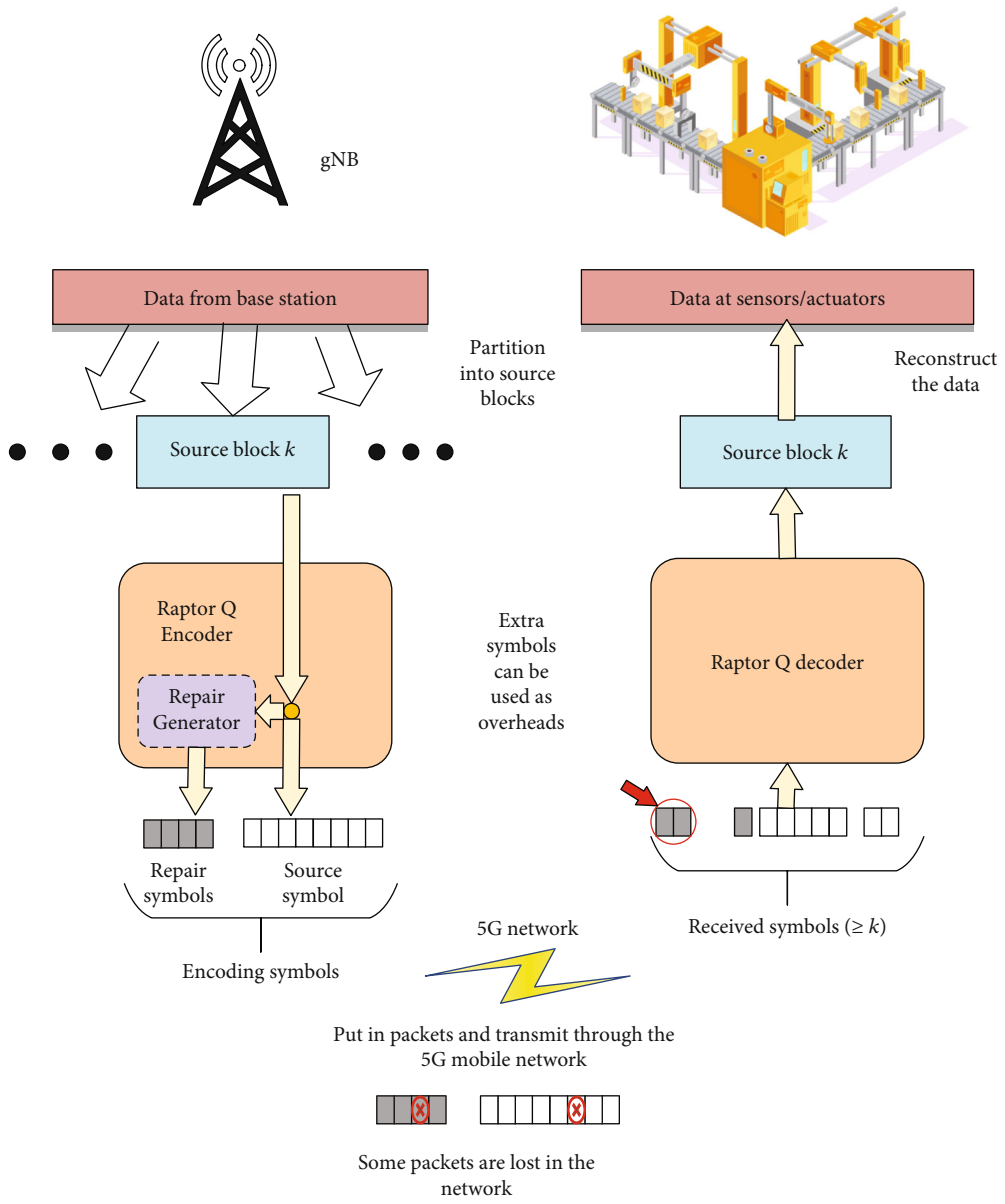

Figure 1: Block illustration of the Raptor Q coding and decoding system.

code as the precode and an inner LT code. With a reasonable code length, R10 code may efficiently disseminate data over a broadcast/multicast network [7]. As a result, rateless codes for the mMTC have the potential to provide excellent reliability [8]. One approach for addressing this problem is to use the most recent rateless codes, such as Raptor Q codes with maximum likelihood (ML) decoding algorithm [9, 10], to enhance coding performance for delivering delay-sensitive applications across future 5G networks. Raptor Q codes are a high-order field F_q extension of Raptor codes that is seen as a promising option to enhance the capacity of R10 codes, providing a compromise between complexity and reliability. The 3GPP has standardized the Application Layer Forward Error Correction (AL-FEC) based on Raptor codes [5] over Multimedia Broadcast and Multicast Services (MBMS) [11] to offer robust and dependable multicast/broadcast services over unreliable channels. Raptor codes were adopted by the 3GPPP because they outperformed previous AL-FEC schemes and because they are implemented in software rather than hardware. Furthermore, the quantity of redundant symbols may be calculated on-the-fly, removing the need for exact channel information prior to data transmission. Because multicast/broadcast transmission is without an ARQ mechanism, the AL-FEC technique sends redundant data together with the original data (packets) to allow the receiver to recover damaged or missing source data by utilizing the redundant ones.

For broadcast and multicast services via wireless networks, AL-FEC protection based on Raptor codes has been widely investigated. These studies investigated the tradeoffs between AL-FEC, physical, and MAC layer parameters

for broadcast services over WLANs [12, 13], Long-Term Evolution (LTE) [14, 15], and Digital Video Broadcasting-Handheld (DVB-H) [16] and found that only a well-designed and optimized system can maximize spectral efficiency and user's QoE. Some research has been conducted into cross-layer optimization frameworks that modify AL-FEC redundancy based on the physical layer modulation and coding schemes (MCSs) used to enable dependable video streaming applications across unreliable wireless channels [17–21]. However, because each multicast user has a different channel condition, multicast video broadcasting to numerous viewers poses extra limitations. As a result, finding system settings that are optimum (offer high quality of experience (QoE)) for each multicast user based on the quality of service (QoS) needs of the applications is difficult.

Hence, the researchers in [22] examined the performance of an AL-FEC protection system in next-generation mobile networks. Findings in [22] demonstrate that the suggested online technique can perform as well as or better than a retransmission-based error recovery technique under certain situations. Meanwhile, researchers in [23] proposed a new AL-FEC application architecture scheme based on Raptor Q codes. Therefore, we investigate the performance improvements that such an error control architecture may bring to NGMN-edge computing integrated systems. The literature has previously looked at industrial applications and their needs for industrial wireless communication systems. In this regard, the work carried out within the German research framework "Reliable Wireless Communication in Industry" should be highlighted. Associated applications were gathered, and their needs merged into three so-called requirement profiles as part of the HiFlecs project [24]. Corresponding needs were gathered from all ZDKI projects and scientifically evaluated by an associated research study [25].

In addition, the whitepaper [26] provided an overview of the use of radio systems in industrial contexts and a summary of the requirements for the various applications. For discrete manufacturing applications, high reliability (PER $\leq 10^{-9}$) and low latency (order of magnitude: 1 ms) are forecasted as stated in [26]. The packet size is intended to be between 20 and 50 bytes. This use case is the most difficult from a communication technology standpoint and is thus taken to be a reference use case in the following without restricting the generality. In terms of industry standardization, the specifications of 3GPP MBMS [11], DVB AL-FEC [27], and IETF FEC framework [28] all contain a common FEC framework to secure streaming service delivery based on AL-FEC. Meanwhile, the researchers in [29] introduced the utilization of fountain codes with very short packets. However, it only investigates the PHY layer without considering the upper layer, such as MAC and APP layer.

Systematic network coding [15–18] is an alternate strategy to reducing computing complexity, which sends the original packets in uncoded form and inserts a limited number of encoded packets into a generation to adjust for network transport inefficiencies. The other key approach to minimize the computational cost of the RLNC is to use sparse coding coefficient rows, which have a relatively modest mandated number of nonzero coding coefficients.

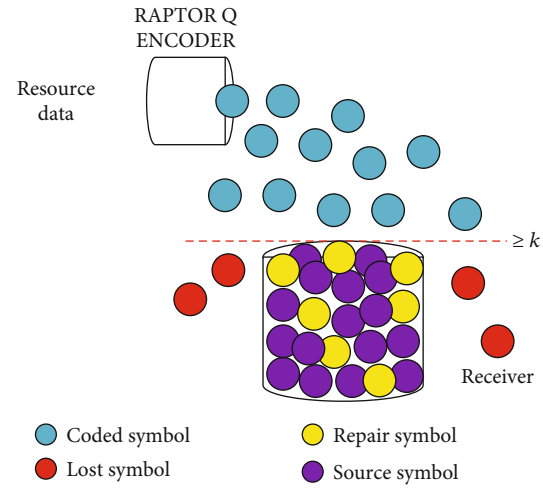

Figure 2: Illustration of symbols in the encoding and decoding system of the Raptor Q codes.

Small Galois fields [19, 20] or novel kinds of network coding [21] have been used in several research investigations to alleviate the computational challenges of network coding. On servers with a high number of graphics processing units (GPUs), the GF (2^8) RLNC can be computed quickly [22–24]. On general-purpose multicore CPUs, computational solutions for GF (2^8) network coding have mostly focused on intelligently splitting the coefficient and data matrices to permit parallel processing [25, 26]. The network coding computations have been substantially accelerated due to these partitioning schemes (and reduced the energy consumption [27, 28]). The matrix block operations can be scheduled according to the dependence structure of the calculations in a DAG [29] to gain some extra performance. Most of the partitioning techniques [25, 26] are suited for progressive RLNC decoding. However, the DAG approach in [29] is confined to nonprogressive decoding of a whole generation of coded packets. Researcher in [29] presented to use the advantages of DAG scheduling to progressive RLNC decoding.

As mentioned in [19, 30–32], the compute-and-forward paradigm, which recodes packets in intermediary network nodes, gives way to RLNC. RLNC can operate on source packet blocks or a sliding window encompassing several source packets [20, 21, 33–36]. DSEP Fulcrum was developed by a researcher in [Nguyen] as a block code that relies on RLNC block coding. However, RLNC comes with high computational complexity. To achieve low computational complexity, a smaller Galois field [37–41] can be considered to minimize RLNC computational complexity at the tradeoff of reduced decoding probability due to the greater probabilities of linearly dependent encoded packets. In addition, the Fulcrum RLNC technique allows for flexible recoding and decoding in either a small Galois field (at the price of collecting more coded packets to compensate for linear dependencies) or a large Galois field (with high complexities) or a mix of the two [42].

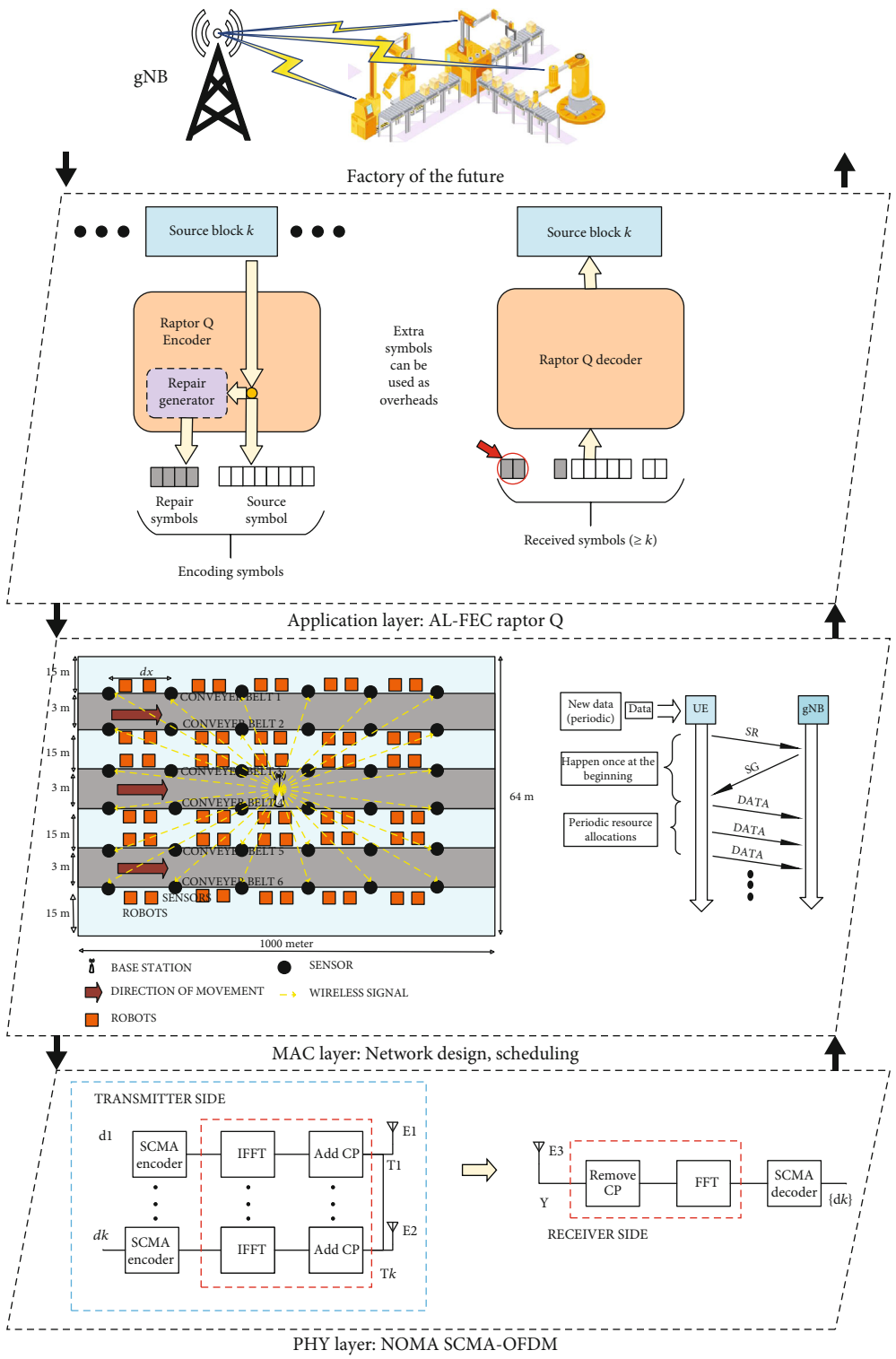

Figure 3: Illustration of the components of the subsystem.

Nonetheless, RLNC also can be replaced with other common rateless coding classes as LT codes [10] or Raptor codes [5]. Raptor codes, in fact, deliver near-optimal performance while requiring substantially less decoding complexity, allowing for longer source blocks. According to [43], Raptor offers codes considerably greater encoding throughput for bigger generation sizes, as investigated in depth in [44], due to a linearly rising asymptotic encoding computational

Table 1: Simulation parameters of the system PHY-MAC-APP [43, 45, 50].

Parameters	Values
PHY layer block	
Radio access mode (modulation)	Sparse code multiple access (SCMA)
SCMA codewords	4
SCMA codebook size	4
SCMA layers	6
SNR	1 : 20
Channel coding (FEC)	Polar
Bandwidth (kHz)	200 (NB-IoT)
Code rate	1/2
Subframe time (ms)	1
Channel model	Rayleigh fading +AWGN
Receiver type	MMSE
Carrier frequency (GHz)	3.5/28
Subcarrier spacing (kHz)	60
Symbol duration (μs)	16.67
Cyclic prefix (μs)	1.17 (normal) 17.84 (extended)
Diversity	Frequency
Subframe (ms)	0.2
Slot (ms)	0.25
Physical channel name	UL
Data rate (kbps)	8.4
Jitter (μs)	100
Delay spread (DS) $\mathrm{lgDS} = \log_{10}(\mathrm{DS/1\ s})$	-1.71 (μ_{lgDS}) 0.18 (σ_{lgDS})
AOD spread (ASD) $\mathrm{lgASD} = \log_{10}(\mathrm{ASD}/1^\circ)$	1.56 (μ_{lgASD}) 0.25 (σ_{lgASD})
AOA spread (ASA) $\mathrm{lgASA} = \log_{10}(\mathrm{ASA}/1^\circ)$	1.66 (μ_{lgASA}) 0.28 (σ_{lgASA})
Shadow fading (SF) [dB]	4.32
K-factor (K) [dB]	7 (μ_K) 8 (σ_K)
MAC layer block	
Numbers of sensors	48
Numbers of robotics/lane	25/50/100
Traffic model	Periodic
BS transmit power (dBm)	30
Noise figure (dB)	9
Payload size (bytes)	50/200/300/500
Speeds (for moving robotics) (km/h)	0(static)/3/7/10
Number of lane	6
Lane width (m)	1
Simulation area size (m)	$1000 \times 64 \times 12$
Queuing model	M/G/1
Rate of arrival	Poisson distributed
Dispatching scheme	First come, first serve
Scheduling	Semi-persistent
APP layer block	
Generation size, T	1024
Total upper layer header, L	23
Source block length, K	20
Code rate, CR	0.5
Base station height (gNB), m	10
FEC	Raptor Q/Repetition/ RLNC

difficulty in n; in contrast, RLNC encoding computational complexity scales asymptotically with $O(n^2)$. It is vital to remember that Raptor does systematic encoding, which means that the n source packets can be delivered in the uncoded form initially as soon as they become accessible from the application, followed by the coded repair symbols.

Although all these previous works used RLNC network coding and FEC codes in the system, none of them focused on the overall performances in terms of packet reception rates (PRR) and the end-to-end (E2E) delay of the system by using the more practical version Raptor codes, which are Raptor Q codes. The emergence of 5G technologies and the Internet of Things (IoT) for Industrial Revolution 4.0 in an indoor smart manufacturing setting is the primary motivation for this research. Smart factory concepts need the use of data from the production line. One way to wirelessly gather machine sensor information in severe manufacturing conditions is an enabler for such applications, and Raptor Q coding has been offered as a tool to develop appropriate network protocols. Hence, this paper presents a cross-layer E2E system performance analysis using Raptor Q codes for an indoor factory of the future. We compare the end-to-end latency and packet reception rate (PRR) of Raptor Q codes encoding and decoding with RLNC network coding for an additional viewpoint on the Raptor Q codes encoding and decoding. More specifically, the main contributions of this paper are presented as follows:

(1) This paper is the extended work from [30] where the authors investigated and designed the PHY-MAC cross-layer model by introducing the NOMA technique at the PHY layer and utilizing semi-persistent scheduling at the MAC layer in an indoor factory scenario. However, the proposed work in [45] had only been investigated until the MAC layer and not entirely investigated until the system/application level of the indoor factory. Hence, this paper focuses on the APP layer performance analysis by introducing Raptor Q codes to improve the overall reliability and end-to-end delay by tackling the packet losses

(2) Adjusting Raptor Q encoding parameters including code rate, symbol size, and the amount of source symbols on the fly to account for time-varying wireless networks and the reliability of Raptor Q codes

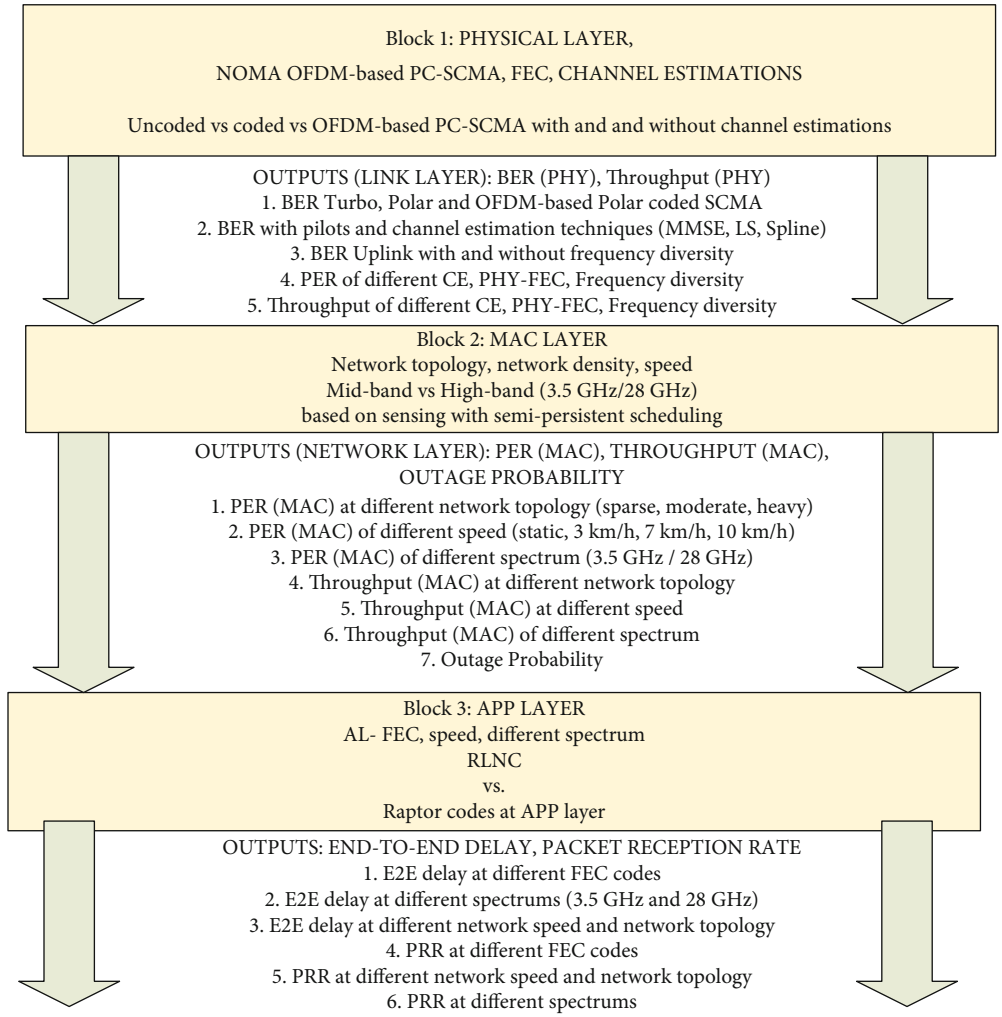

Figure 4: Factory of the future communication model system.

(3) The system model is developed based on cross-layer simulation of potential wireless deployment for future factory automation applications with considered system parameters based on 3GPP TR 38.913 [46] and METIS [47] under different network densities, speeds, and frequency spectrums

(4) An event-based simulator in measuring packet reception rate (PRR) and E2E delay performance is being developed, and the results obtained are analyzed with Repetition codes as the performance comparison. The results could be a valuable insight for the factories of future services [48].

This paper has the following structure. The basic concepts and overview of Raptor Q codes are discussed in Section 2. The PHY-MAC-APP layer simulation system and measurement setup are elaborated in Section 3. Results and discussions are further analyzed in Section 4. Finally, Section 5 presents the conclusion of the paper.

2. Factory Applications and Its Communication System Requirements

The Raptor is a forward error correction (FEC) technique deployed in software that protects against network packet loss at the application layer. A Raptor code is made up of an outer code (precode) Φ and an inner LT code C that are serially concatenated. The precode Φ is a (n, k) block code that uses k source symbols to create n intermediate symbols. The LT code C is then used to create k output symbols by encoding the n intermediate symbols with a $(k\gamma, n, \Omega(x))$ LT encoder, where the inverse of the Raptor code receives code rate CR. The code rate CR is derived as [49]:

$$CR = \frac{1}{\gamma} = \frac{1}{1+\varepsilon}, \tag{1}$$

where $\mathcal{E}$ is the overhead of the Raptor code. Meanwhile, the LT code generator matrix is built using a predetermined

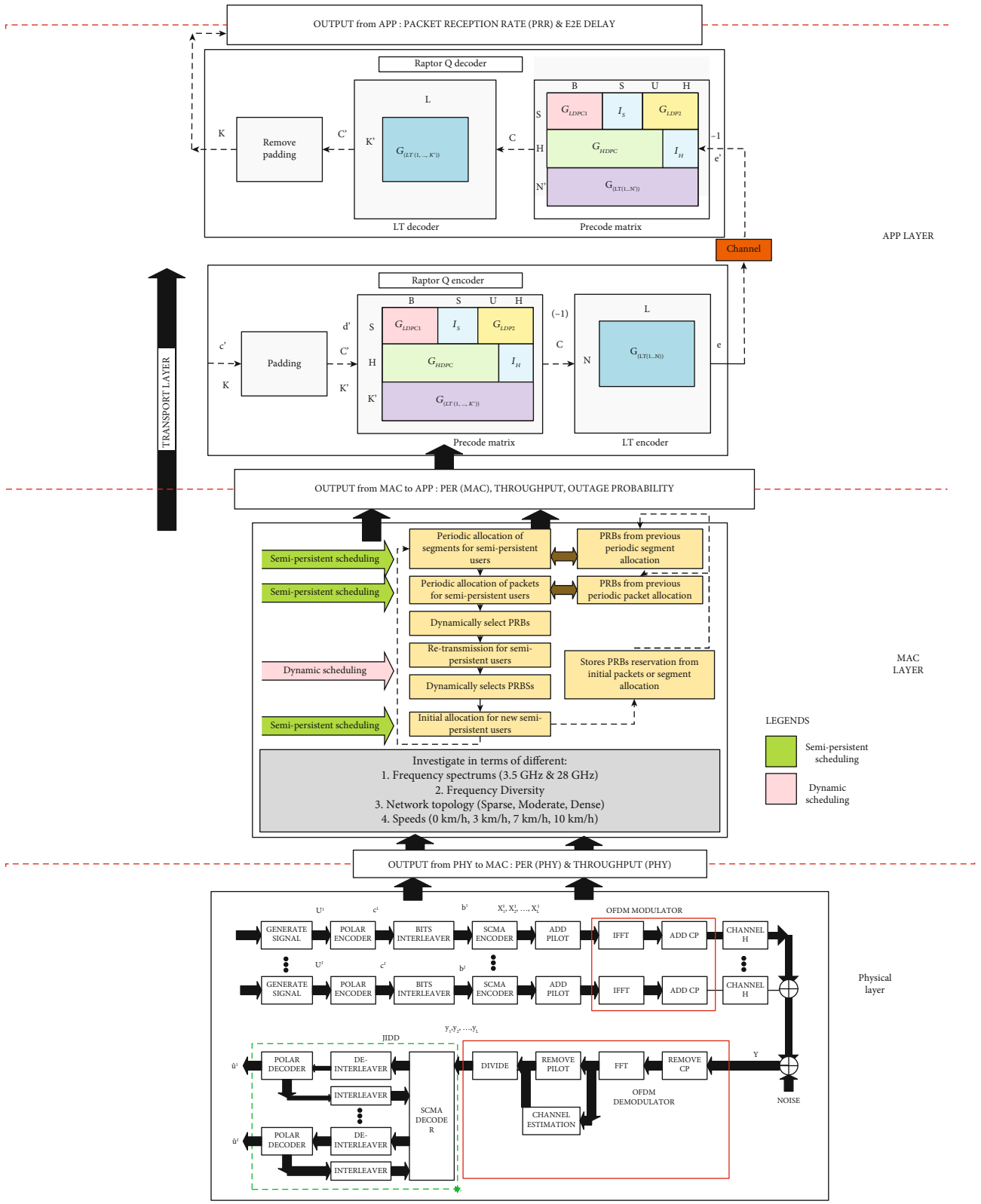

Figure 5: The PHY-MAC-APP system model proposed in this paper.

degree distribution expressed as

$$\Omega(x) = \sum_{d=1}^{d_{\max}} \Omega_d x^d, \tag{2}$$

where each row's degree d follows the probability distribution in (3) and satisfies (4).

$$\Omega_d = (\Omega_1, \Omega_2, \cdots, \Omega_{\max}), \tag{3}$$

$$\Omega(x) = \sum_{d=1}^{d_{\max}} \Omega_d = 1. \tag{4}$$

The Raptor code is denoted as (5), whereas the information symbols and received coded symbols are denoted as

$$\eta = \xi(\gamma, k, \Omega(x), \Phi), \tag{5}$$

$$\boldsymbol{s}_{k\,x\,1} = (s_1, s_2, s_3, \cdots, s_k)^T, \tag{6}$$

$$\boldsymbol{c}_{\gamma k\,x\,1} = \boldsymbol{G}^{LT}_{\gamma k\,x\,n} \boldsymbol{G}^{pre}_{n\,x\,k} \boldsymbol{s}_{k\,x\,1}, \tag{7}$$

where k represents the number of information symbols, γk is the number of received symbols, and n denotes the number of intermediate symbols. The LT generator matrix and the precode generator matrix, respectively, are denoted as $\boldsymbol{G}^{LT}_{\gamma k\,x\,n}$ and $\boldsymbol{G}^{pre}_{n\,x\,k}$. Moreover, the input alphabet of a q-ary Galois Field, $\boldsymbol{G}^{F(q)}$, is expressed as

$$\boldsymbol{G}^{F_q}_{q-1} = \left(0, 1, \alpha, \cdots, \alpha^{q-2}\right), \tag{8}$$

where α is denoted by a primitive element of GF(q) and then the Raptor Q code's nonzero elements are then arbitrarily selected from $\boldsymbol{G}^{F_q}_{q-1}$, where each nonzero entry in $\boldsymbol{G}^{LT}_{\gamma k\,x\,n}$ and $\boldsymbol{G}_{n\,x\,k}$ is sampled separately and uniformly from F_q.

Raptor Q is the most versatile and recent technology in Digital Fountain's Raptor range [10]. At the application layer, the Raptor Q encoder collects incoming Real-time Protocol (RTP)/User Datagram Protocol (UDP) packets to build source blocks, each of which has k source packets (symbols) with T bytes, and then creates N encoded symbols with T bytes from each block. Because the Raptor Q codes are systematic, the original k source symbols are the initial encoding symbols of N encoded symbols, and the remaining R symbols of N symbols are termed as the repair symbols $(N = k + R)$. The $CR = k/N = k/(k + R)$ code rate for Raptors is expressed as (1). Meanwhile, the Raptor Q decoder waits for all UDP packets belonging to a specific source block to arrive at the receiver. When the total number of acquired packets (source and repair symbols) for a particular source block is $k^{'}\,(\mathcal{E} + 1)\,k$ at the decoder, the Raptor Q decoder can decode the block with a high probability where all source packets of the source block are rebuilt and sent to the application layer.

Figure 1 shows a simpler illustration of the concept of signals from the gNB emitted at the application layer in a factory environment. The data sent from gNB is then divided into several source blocks k. This source block is encoded using Raptor Q encoding, which produces a source symbol followed by a repair symbol generated by the repair generator. These encoded symbols are arranged in packets and transmitted over the 5G mobile network. In the network, some transmitted packets are lost due to interference of the surrounding conditions as well as poor or challenging environment. On the sensors/actuators decoding section, the received symbol must be $\geq k$. The redundant repair symbol can be used as an overhead for the source symbol in the Raptor Q decoding process at the sensors/actuators. The source block data on decoding then reconstructs the data. Then, the data is sent to the receiver. In the use of the Raptor Q code, the symbols do not need to be arranged sequentially. Most importantly, sufficient symbols should be received at the receiver, as illustrated in Figure 2.

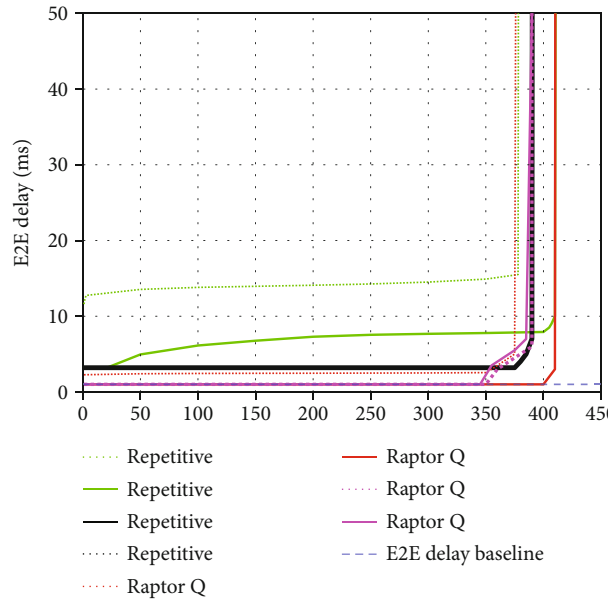

Figure 6: E2E delay in perfect CSI.

3. System Model

An event-based simulator is developed to analyze the end-to-end system performance of a 5G wireless communication system for an indoor factory of the future across different cross-layer system parameters. The simulator has been developed and divided into three subsystems, as shown in Figure 3 to decrease computing complexity and time. The components of the subsystems consist of the following:

(1) *Physical layer:* nonorthogonal multiple access (NOMA)-based OFDM-SCMA [50]. SCMA combines the bit-to-QAM symbol mapping and spreading procedures, and entering bits are immediately mapped to a multidimensional codeword of an SCMA codebook set

(2) *MAC layer:* indoor factory cross-layer design simulator as proposed in work [45] where the results obtained from [45] are to be used and analyzed

further in the APP layer simulator to evaluate overall system performance

(3) *Application layer:* AL-FEC Raptor Q model simulator as proposed in this paper

The indoor factory broadcast concept is based on [48], where it enables a simple, rapid, and large-scale transmission of messages without feedback to the sensors/actuators. It eliminates the need for complicated routing and avoids coverage limitations by reducing reliance on high-cost infrastructure rollout. The objective of this indoor factory broadcast model is to evaluate the latency and reliability of AL-FEC Raptor Q codes and Repetition codes in an indoor factory building (consisting of sparse, moderate, and dense network density) contexts for the same scenario. This indoor factory broadcast model is a MATLAB-based event-based simulator that comprises three distinct components. Meanwhile, RLNC simulation is based on [51] theory and is implemented in our in-house simulator from the PHY layer until the APP layer.

The location of each sensor is examined and assessed using the position, speed, and outputs of the realistic sensor density (v_d) for each beacon period to build an indoor factory simulator, as illustrated in Figure 3. Each sensor's (or actuators) received power P_R is computed based on its distance from the tagged sensor. The SINR (signal-to-interference ratio) is calculated for each sensor based on co-channel interference from a list of sensors with $P_R >$ threshold.

A NOMA OFDM-SCMA simulator is utilized in the physical layer block to compute the BER_{phy}, PER_{phy}, and $throughput_{phy}$ for various SNR (signal-to-noise ratio) values. The computed SINR is transmitted to the (PER_{PHY}) versus SNR curves for each sensor or actuator. The component parameters in the PHY layer are considered in Table 1.

The MAC system model has been explained in our previous work in [45]. To summarize, a cross-layer design for an indoor factory of the future is designed and developed to suit the stringent requirements for URLLC. In work [45], a cross-layer strategy is proposed by utilizing semi-persistent scheduling (SPS) at MAC and code-domain NOMA at PHY to achieve an ultra-reliable communication (URC) for potential 5G mobile network deployment for the factory of the future. By having outputs from [45], results of PER_{mac}, $throughput_{mac}$, and outage probability are critically evaluated and analyzed by varying multiple parameters such as network densities (sparse, moderate, and dense), various speed of sensors/actuators that are realistic to the indoor factory scenarios (static, 3 km/h, 7 km/h, and 10 km/h), and two allocated 5G frequency spectrums, which is mid-band (3.5 GHz) and high band (28 GHz).

The reason for using two different types of spectrums at MAC layer is to investigate the characteristics of the spectrums when it is deployed in an indoor factory. Based on the results in [45], it is shown that the mid-band spectrum outperformed the high band due to the high-band spectrum being highly susceptible to the clutters present in the factory. The traffic model considered in the MAC layer block is periodic since SPS is utilized in the MAC layer; it has the advantage of manipulating the previous knowledge regarding the traffic characteristics. Moreover, the first-come first-serve (FCFS) dispatching scheme is considered, and it is assumed that no items are discarded from the queue. A M/G/1 queuing model is considered, and the rate of arrival is classified as Poisson distributed. In addition to that, general distribution is assumed as a service rate. Table 1 shows the parameters used at the MAC layer block, as stated in [45], whereas Figure 4 shows the factory of the future communication model system.

To increase the reliability of the indoor factory broadcast system model, the AL-FEC model is employed. The FEC block emulates this function in the simulation. A source block (SB) is formed of K source symbols of size $T = (N_{PSDU\,FEC})$ in the FEC block. The physical layer service data unit (PSDU) size for a particular message type is $(N_{PSDU,FEC})$, and FEC is described as

$$\left(N_{PSDU,rep}\right)_{app} = N_{payload} + N_{headers}, \tag{9}$$

$$\left(N_{PSDU,rap}\right)_{app} = \left(\frac{N_{payload}}{k}\right) + N_{headers}. \tag{10}$$

There are three types of FEC schemes introduced in this paper, which are the Repetition codes, RLNC, and Raptor Q codes that are implemented at application layer (APP). Repetition codes are introduced as it is simple and there are no feedback requirements. The complexity of this method is minimal. Repetition codes, on the other hand, have a high latency requirement and inefficient bandwidth usage, making them unsuitable for URLLC applications.

As a result, this paper investigates the systematic Raptor Q codes, and the results obtained are being compared to the Repetition codes and RLNC results. The overall PHY-MAC-APP model system is shown in Figure 5.

At the application layer, the Raptor Q encoder gathers input SB at the transmitter and fragments them to size $K = 8$ to create source symbols of size $T = (N_{PSDU,rap})_{APP}$. K is the length of a source block or the number of source symbols (SSs) that make up a source block (SB) in raptor codes. It also produces R repair symbols, which are specified by the code rate (CR) in (1). The Raptor decoder gathers all the source symbols that correspond to a given source block at the receiver. If the total number of combined received symbols for a particular block of data meets $k' \geq (\mathcal{E} + 1) * k$, where the encoded symbol overhead $\mathcal{E} > 0$, the Raptor decoder successfully decodes all of the source packets. Each transmitted encoded symbol has an ESI (encoded symbol identifier) sequence number that may be used to calculate the average end-to-end delay.

Note that $CR = 1$ denotes the absence of the redundant symbols, whereas $CR = 0.5$ denotes a 50% increase in overhead. Raptor encoding and decoding delays are less than 1 ms, according to measurements in [49], and Raptor chipsets with fast implementation are widely available. As a result, the Raptor processing delay is ignored when calculating the end-to-end delay. In this model, the User Datagram Protocol (UDP) is assumed for low latency and no retransmissions. For successful decoding (PER <1%), the packet reception rate (PRR) results obtained from Equation (11)

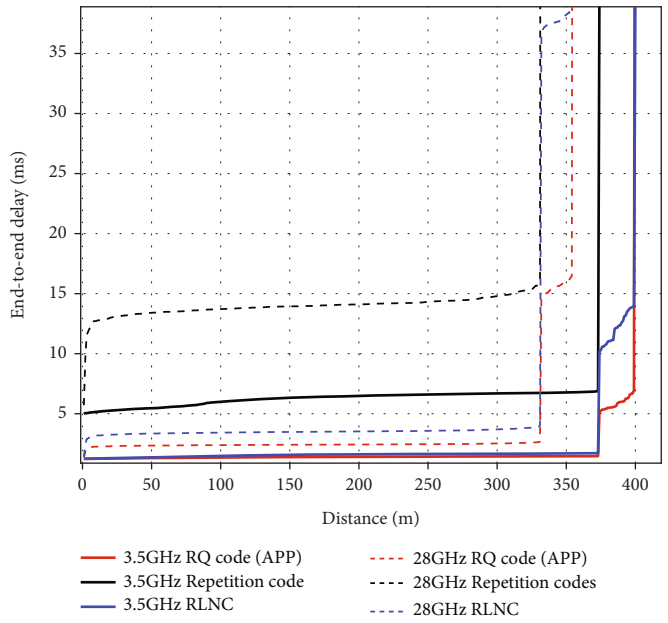

Figure 7: E2E delay with frequency diversity in dense network.

are transmitted to the FEC block, where either Repetition codes overhead $N_r = 4$ or Raptor Q codes overheads $\mathcal{E}$ is chosen depending on the FEC type.

$$\begin{aligned}(\rho(v_d, d)) &= \left(1 - PER_{phy}(s,t)\right), N_{\max} \geq N_{\text{receive}} \\ &= \left(1 - PER_{phy}(s,t)\right) * \left(\frac{N_{\max}}{N_{\text{receive}}}\right), N_{\max} < N_{\text{receive}},\end{aligned} \tag{11}$$

where $N_{\max}$ is the maximum number of sensors/actuators within $r_{\text{sense}} = 100$ m of the transmitter sensor/actuator and N_{receive} is the total number of sensors/actuators that successfully receive the signal among $N_{\max}$; PER_{PHY} is the PHY layer PER calculated in the PHY layer block. In addition, the PRR used in this study is the average PRR of all of the sensors/actuators at a distance of d from the tagged sensor/actuator. For the end-to-end delay computation, the corresponding overhead for the provided FEC type is used. The end-to-end latency is calculated using Equations (12) and (13), with the number of repetitions $N_r = 4$ for Repetition codes and ESI overhead of $ESI_{K+\mathcal{E}} = K/CR$ for Raptor codes.

$$(\tau_{ss}(v_d))_{rep,APP} = N_r * \tau_{MAC}(v_d), \tag{12}$$

$$(\tau_{ss}(v_d))_{\text{raptor}} = \frac{K}{CR} * \tau_{MAC}(v_d). \tag{13}$$

Given the equation $\tau_{MAC}(v_d)$ is expressed as

$$\tau_{MAC}(v_d) = T_s = T_{\text{total}HD}, \tag{14}$$

where $T_{\text{total}HD}$ is the time taken by PHY layer source symbol. It is assumed that a half-duplex $(ksi = 0)$ operation is being used, which corresponds to the full cancellation of the self-interference, and all resources are assumed available $(\delta = 1)$.

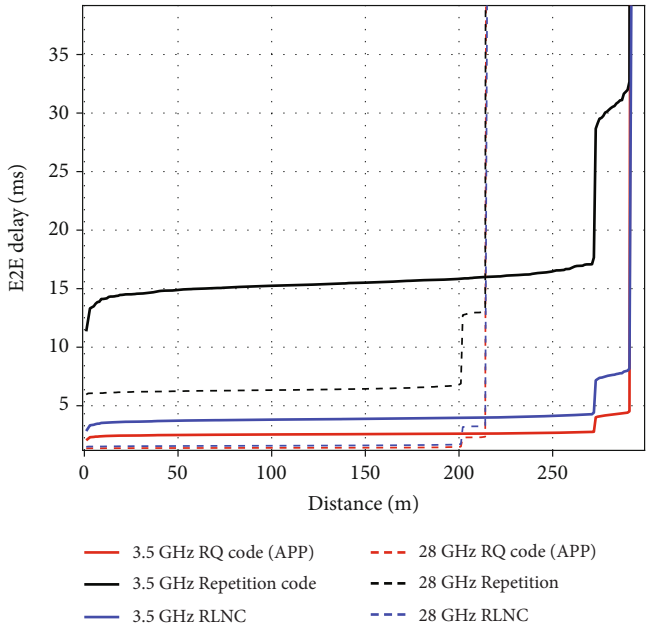

Figure 8: E2E delay without frequency diversity in dense network at stationary.

4. Results and Discussions

In this section, the system performance of factory of the future is developed and investigated in terms of packet reception rate (PRR $(\rho(v_d, d))$) and end-to-end delay in an indoor factory environment. Firstly, the performance of Repetition, RLNC,

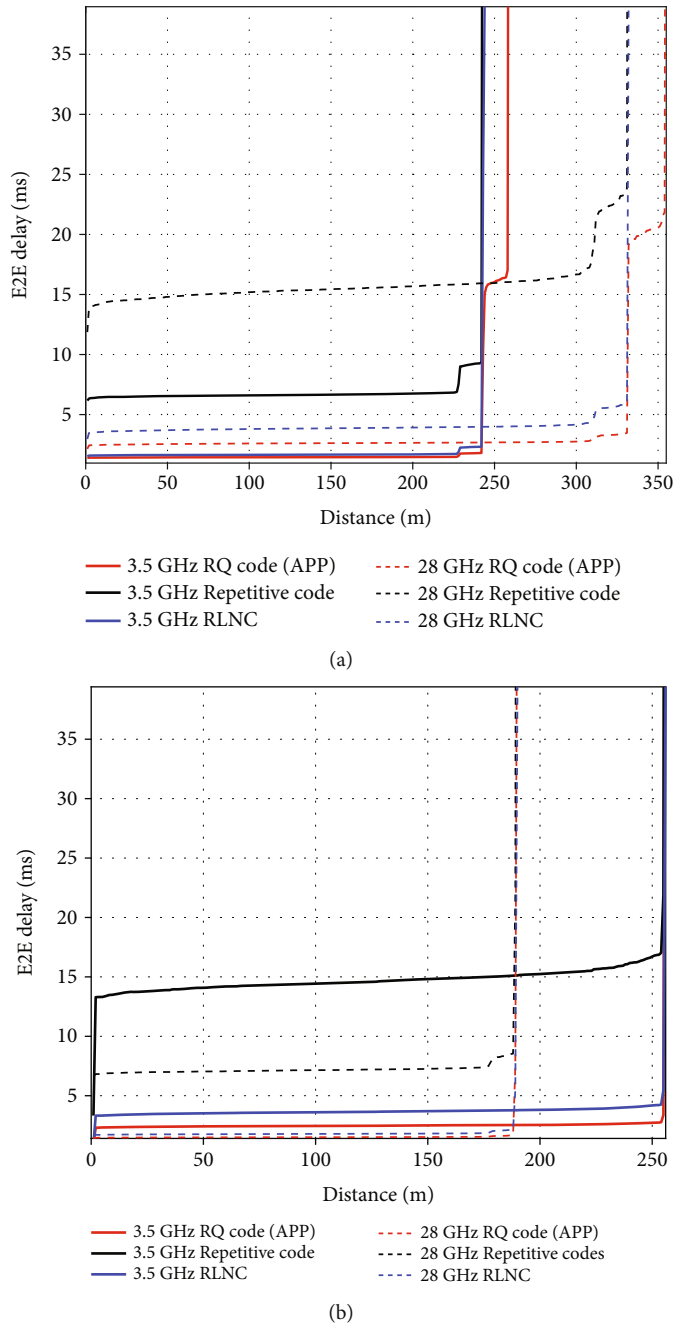

Figure 9: (a) E2E delay at 3 km/h sparse network and (b) E2E delay at 10 km/h.

and Raptor Q codes are being compared in terms of different parameters such as sensor network densities, speeds, and spectrums. Sensor density is calculated as $v_d = 0.025$ sensor/meter for sparse network, $v_d = 0.05$ sensor/meter for moderate network, and $v_d = 0.1$ sensor/meter for dense network as being computed by using Equations (15) and (16). To ensure consistency when comparing both codes, $r_{sense} = R$ is standardized to 100 m, and it is assumed that all resources are available $(\delta = 1)$. Also, half duplex operation $(ksi = 0)$ is used to simulate all the sensors [55].

$$v_d = n \times \frac{N_l}{1000}, \tag{15}$$

$$n = \frac{1000}{6 \times speed}, \tag{16}$$

where N_l indicates number of lanes as per stated in Table 1.

4.1. End-to-End Delay Performance. Based on stringent requirements of URLLC as mentioned in [1], the target

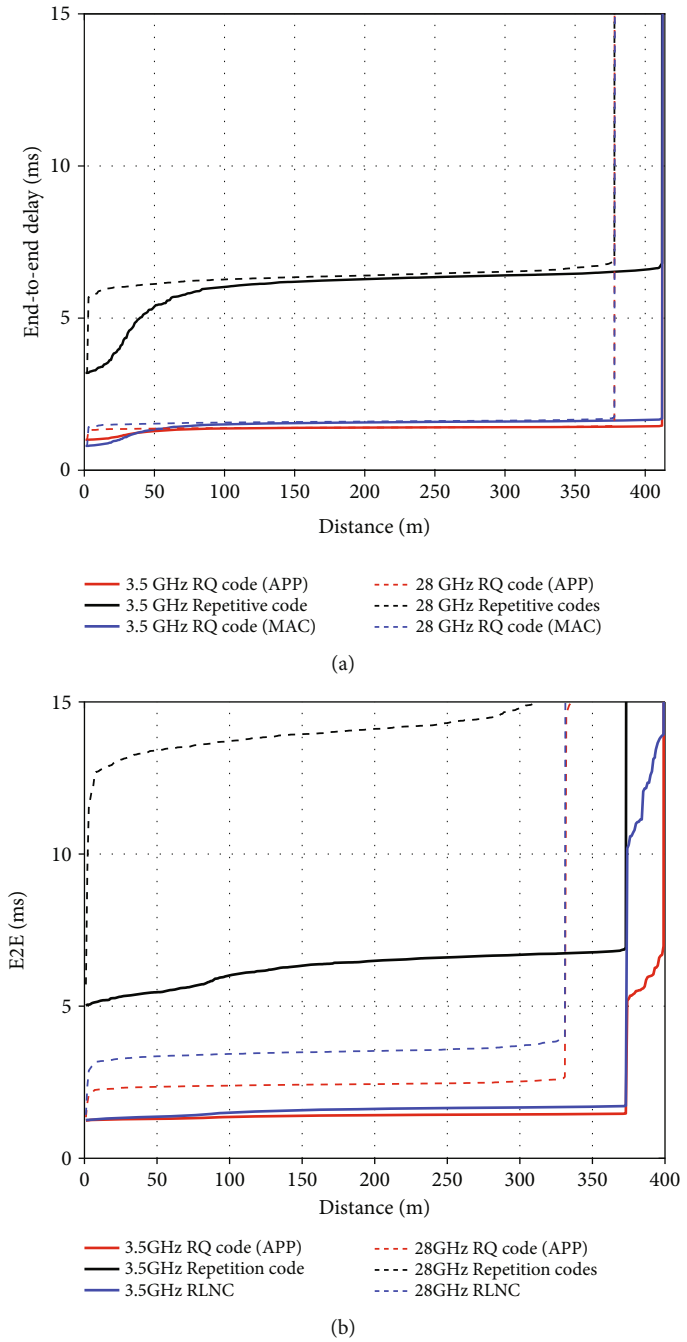

Figure 10: PRR RLNC vs. Raptor Q in moderate scenario at static and 10 km/h.

E2E delay is 1 ms. Figure 6 shows the performance comparison of Repetition and Raptor Q codes in perfect channel state information (CSI). It is shown that AL-FEC Raptor Q for static mid-band with dense network deployment has the results by having an E2E delay of 1 ms for coverage of 400 m. Meanwhile, the same spectrum of 3.5 GHz of Repetition codes has shown the distance coverage of 400 m with larger than 15 ms delay. This shows that it was unable to achieve the target URC E2E delay requirement, which is 1 ms, exceeding a huge delay gap of 7 ms, whereas Raptor Q codes of 28 GHz obtained a distance coverage of 391 m. The performance of the mid-band spectrum gives an improvement of nearly 21 m. The combination of mid-band spectrum and Raptor Q codes at APP provide high tolerance towards packet error channel erasure by extending the coverage. Starting from this point onwards, the performances of source coding are compared between RLNC and Raptor Q and also be considered. Next, the E2E delay results were analyzed at dense network density with frequency diversity, as shown in Figure 7. In this case, the situation is investigated at a speed of 10 km/h. The difference in performance between the mid-band and high band is assessed by

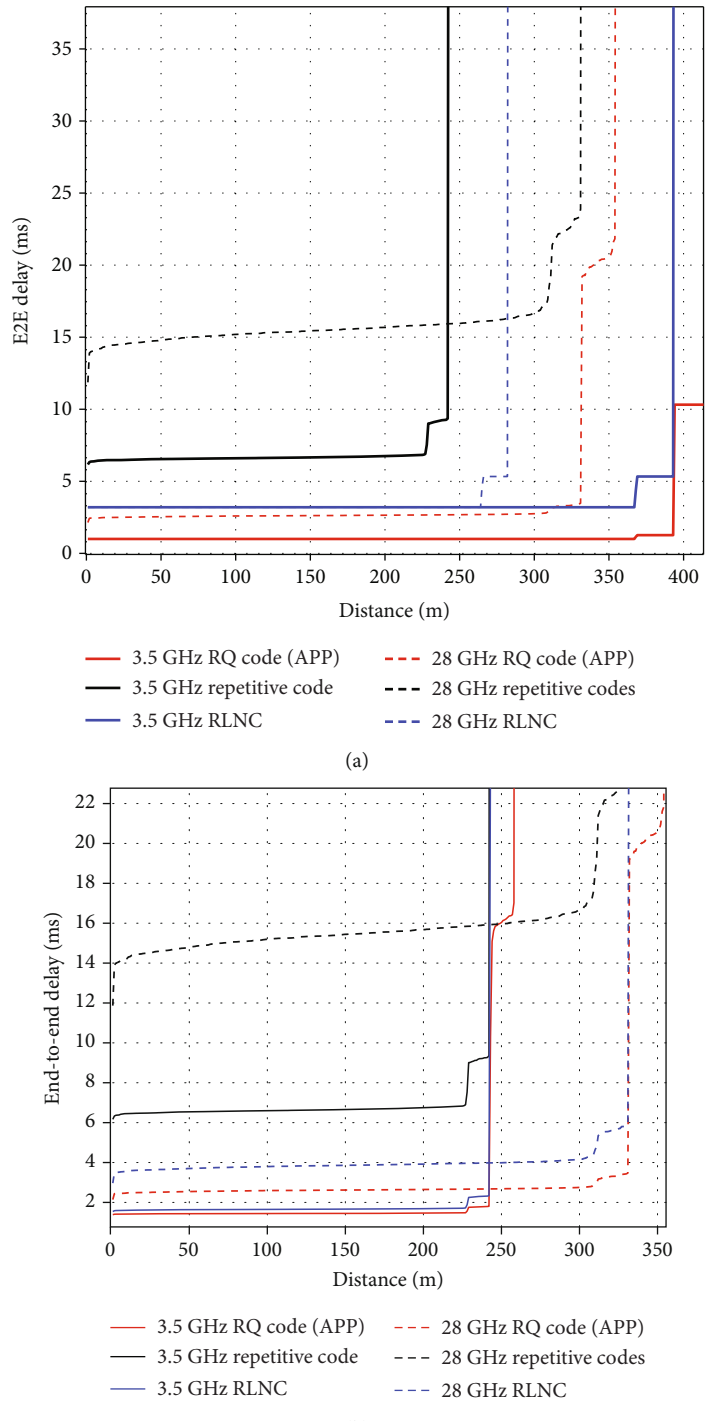

Figure 11: E2E delay in dense network at 3 km/h (b) E2E delay in dense network at 7 km/h.

using RLNC and Raptor Q codes. It can be seen that at 3.5 GHz with dense network density and Raptor Q codes yield the best results compared to the rest. It covers a distance of 375 m at an E2E delay of 1 ms. Meanwhile, the same spectrum of RLNC codes also yields the same distance coverage as Raptor Q. Furthermore, based on the overall performances, it can be seen that the mid-band outperformed the high band. This is because the characteristics of the 3.5 GHz band are more stable and robust towards longer distance coverage during movement, whereas, the high-band signal (28 GHz) is highly susceptible to obstructions and signal interferences.

In addition to that, Figure 8 shows the performance comparison of E2E delay without frequency diversity. The performance of the simulation is assessed similarly in Figures 6 and 7. As predicted, the mid-band with Raptor Q codes at stationary

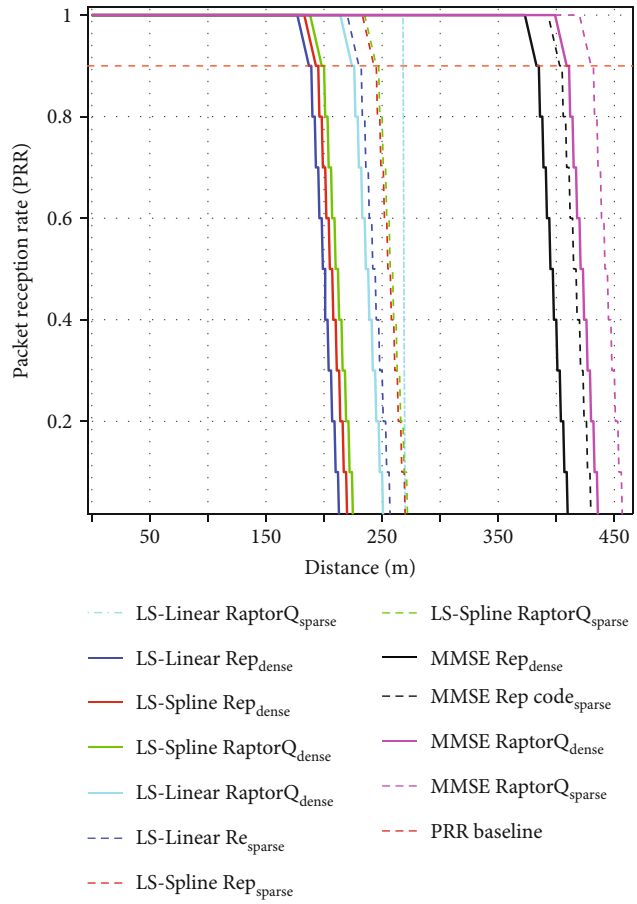

Figure 12: PRR comparison between types of channel estimations.

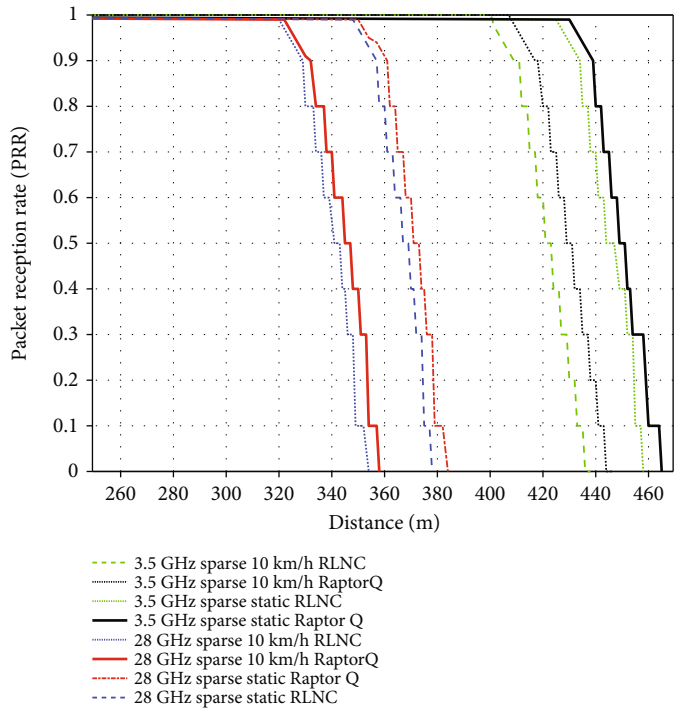

Figure 13: PRR in sparse scenario at static and 10 km/h.

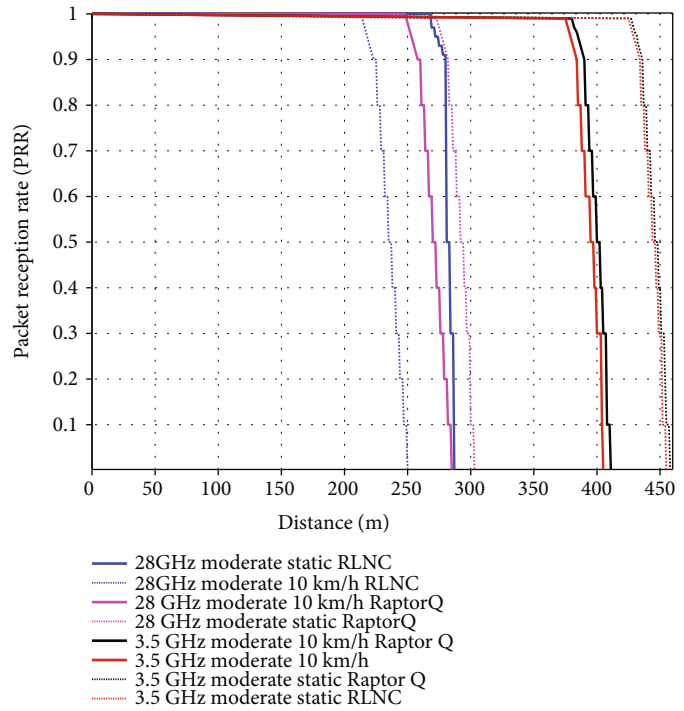

Figure 14: PRR RLNC vs. Raptor Q in moderate scenario at static and 10 km/h.

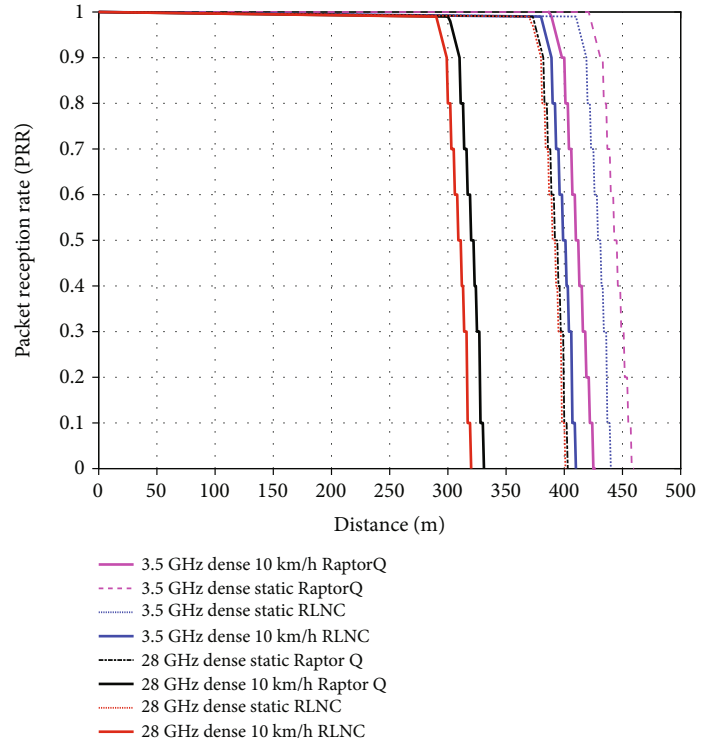

Figure 15: PRR RLNC vs. Raptor Q in dense scenario at static and 10 km/h.

Table 2: Coverage performance between RLNC and Raptor Q codes at 3.5 GHZ for different speeds and network densities.

Distance coverage		Speed			
Targeted PRR = 0.9	Density	Static	3 km/h	7 km/h	10 km/h
	Sparse	426 m	410 m	405 m	402 m
RLNC	Mod.	425 m	409 m	402 m	395 m
	Dense	410 m	405 m	390 m	380 m
	Sparse	430 m	420 m	412 m	407 m
Raptor Q codes	Mod.	427 m	412 m	410 m	399 m
	Dense	422 m	409 m	400 m	387 m
	Sparse	5 m (0.93%)	10 m (2.4%)	7 m (1.7%)	5 m (1.2%)
Improvement (meter)	Mod.	2 m (0.47%)	3 m (0.73%)	8 m (2.0%)	4 m (1%)
	Dense	12 m (2.8%)	4 m (1.0%)	10 m (2.5%)	7 m (1.8%)

Table 3: Coverage performance between RLNC and Raptor Q codes at 28 GHz for different speeds and network densities.

Distance coverage		Speed			
Targeted PRR =0.9	Density	Static	3 km/h	7 km/h	10 km/h
	Sparse	357 m	355 m	340 m	320 m
RLNC	Mod.	280 m	238 m	230 m	250 m
	Dense	370 m	311 m	315 m	300 m
	Sparse	361 m	378 m	370 m	322 m
Raptor Q codes	Mod.	283 m	242 m	233 m	260 m
	Dense	373 m	320 m	322 m	290 m
	Sparse	4 m (1.1%)	23 m (6.0%)	30 m (8.8%)	2 m (0.6%)
Improvement (meter)	Mod.	3 m (0.7%)	4 m (1.7%)	17 m (7.3%)	10 m (3.9%)
	Dense	3 m (0.8%)	9 m (2.8%)	7 m (2.2%)	10 m (3.4%)

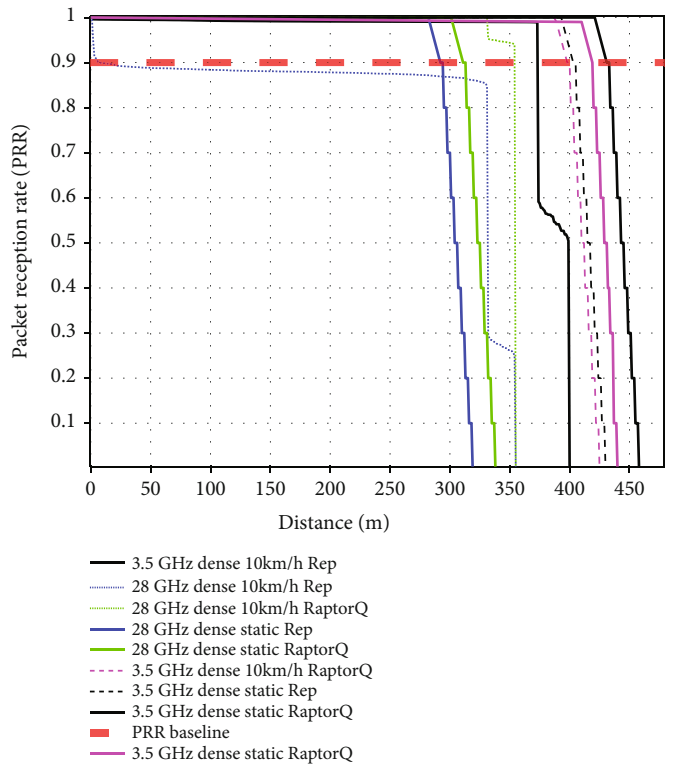

Figure 16: PRR Repetition vs. Raptor Q in dense scenario at static and 10 km/h.

showed the best results, with the distance coverage of 275 m at 1 ms E2E delay. RLNC also yields 275 m coverage; however, the delay is more than 1 ms, where this shows that it was unable to achieve the target URC E2E delay requirement, which is 1 ms. Moreover, the high band with Raptor Q yields a distance coverage of 200 m within acceptable E2E delay. Pursuing this further, Raptor Q codes and RLNC showed an improved distance coverage of 75 m at a stationary position.

Subsequently, the results obtained are analyzed in terms of frequency diversity with the presence of MMSE CE. Figures 9 and 10 are analyzed in different networks at different speeds such as 3 km/h and 10 km/h, respectively. Raptor Q codes with the spectrum of 3.5 GHz, as shown in Figure 9(a) have shown a result, which was 225 m distance coverage at E2E delay of 1 ms, whereas as shown in Figure 9(b), the highest distance coverage by Raptor Q are slightly lower, which was 189 m. There is an increase of 6.4% in the mid-band sparse network at 3 km/h, whereas a 2% increase in high-band sparse at 10 km/h.

In Figure 10(a), static and 10 km/h in moderate scenarios using Raptor Q codes, the distance covered is observed to be 410 m within the targeted 1 ms delay. RLNC, however, is not achieving the URC targeted delay of 1 ms, although it has the same distance coverage as Raptor Q codes. Correspondingly, spectrum 3.5 GHz outperformed spectrum 28 GHz with the distance coverage difference of 100 m at the static condition and 58 m at the speed of 10 km/h. Afterward, Figure 10(b) showed the results of Raptor Q codes and RLNC at 3.5 GHz and 28 GHz spectrums. Raptor Q codes at 3.5 GHz outperformed the Raptor Q codes at 28 GHz by a total distance coverage difference of 75 m. However, at a speed of 10 km/h, only Raptor Q codes with mid-band 5G is achieving the URC-targeted E2E delay. Despite good distance coverage, the rest are not achieving the stringent requirement of URC targeted delay.

Concurrently, the results are being analyzed under a busy and dense network scenario, which is 100 sensors per km per lane. In addition, the results are also being observed at different speeds such as static, 3 km/h and 7 km/h. As expected, the mid-band spectrum outperformed the high-band spectrum in all four scenarios. In a dense network, the transmitted messages are experiencing a high rate of collision with one another which has caused an increase in E2E delay. Raptor Q codes in mid-band managed to achieve results within the targeted E2E delay. In Figures 11(a) and 11(b), at speeds of static and 3 km/h, the coverage area is up to 360 m, whereas the distance coverage is 280 m at speeds of 7 km/h.

4.2. Packet Reception Rate (PRR) Performance. Figure 12 shows the comparison of PRR with different types of CE at the receiver in sparse and dense scenarios. Based on [1], the targeted range for PRR is 0.9. MMSE CE outperformed LS CE by 432 m in distance coverage by implementing Raptor Q codes scheme in sparse networks. Besides, Repetition codes with the MMSE CE scheme also outperformed LS CE by 385 m (dense) and 405 m (sparse), respectively. The rest of the results are observed and analyzed based on MMSE CE at different scenarios, spectrums, AL-FEC, and sensor speed.

As shown in Figure 13, the results show a sparse network condition at speeds of static and 10 km/h, respectively. It is observed that Raptor Q codes at mid-band spectrum at stationary yielded the best result by having a distance of 426 m at $PRR = 0.9$ or 0.93% coverage improvement compared to RLNC, while RLNC of 10 km/h mobility at high band produced the worst results by having a distance of 402 m. This means that the Raptor Q codes scheme showed an improved distance coverage of 5 m or 1.2%.

Consequently, the results are obtained and analyzed in moderate conditions at static and 10 km/h as shown in Figure 14, whereas in Figure 15, the PRR is being analyzed in a dense scenario at static and 10 km/h. In a moderate static network scenario (mid-band), an improvement of 2 m or 0.47% can be observed, whereas at 10 km/h, an improvement of 4 m or 1% can be seen. On the other hand, a coverage improvement of 3 m (0.7%) and 10 m (3.9%) can be observed in the high-band spectrum at static and 10 km/h. Additional repair symbols are sent by Raptor Q codes to compensate for a target PRR's decreased performance. However, the cost associated with the additional repair symbols is relatively high.

Tables 2 and 3 show the summary of the obtained results from Figure 16, Figure 13, and Figure 14. These tables are divided into three categories which are sparse, moderate, and dense network. Based on the overall results in all two tables, it can be observed that the difference in coverage between RLNC and Raptor Q codes at high band is in the dense network at a speed of 10 km/h, which is 10 m or 3.4% improvement. Meanwhile, in mid-band, the improvement of 7 m or 1.8% can be seen. This is because the Raptor Q codes have a high tolerance for packet errors as well as erasure channels. Each packet is believed to have an equal chance of error, and if a mistake occurs, the packet is expected to be "erased." Since the packet transmission at higher layers has the same characteristics as a binary erasure channel (BEC), thus, it is able to offer a good opportunity for the execution of Raptor Q codes.

5. Conclusion

In this paper, the performance of PRR and E2E delay is evaluated and analyzed by using two types of AL-FEC schemes, namely, RLNC and Raptor Q codes, as a comparison. To test the reliability of such codes, performance is tested in various scenarios such as network density, sensor's velocity, and different spectrums (3.5 GHz and 28 GHz) which are studied and analyzed.

Firstly, the delayed performance has shown that the Raptor Q codes are able to meet the strict URC requirement of 1 ms in all types of proposed scenarios (sparse, moderate, and dense). The Raptor Q codes also meet the 1-ms delay target in a static state as well as in a moving state of 3 km/h, 7 km/h, and 10 km/h. In contrast to the RLNC, wherein some scenarios, its performance is not able to meet the pre-determined URC requirements. This clearly shows that the Raptor Q codes are ideal for obtaining low latency times at the APP layer. It is crucial to remember that Raptor Q executes systematic encoding, which means that the n source packets can be delivered in the uncoded form initially when

they become available from the application, followed by the y-coded repair symbols.

Besides that, the results are evaluated at the packet reception rate (PRR). In the attached results, the Raptor Q codes are not only able to give good results (PRR = 0.9) of 1.2% in a high-density static scenario and 1.8% in high density 10 km/h mobility (mid-band), even the Raptor Q codes are also able to meet PRR = 0.9 in the mobility scenario at 10 km/h in dense network with the improvement of 3.4% or 10 m in distance coverage in the 5G high band. Achievable PRR indicates that the communication system is robust and highly reliable in packet delivery in the application layer. Meanwhile, the RLNC cannot meet the requirement of PRR = 0.9 in the dense scenario at a speed of 10 km/h. These results imply that the Raptor Q calculation for low overhead encoding and decoding for all generation sizes, n, will be significantly faster if the implementation has been tuned for the scenario when the number of symbols needed to construct the intermediate block is near to n. Furthermore, Raptor Q decoding performance is significantly greater than RLNC decoding throughput because Raptor Q has a linear asymptotic decoding difficulty, whereas RLNC decoding has an underlying asymptotic computational complexity of $O(n^3)$.

However, this paper only focuses on a specific generation size and symbol size setting for an indoor factory. As future work, it is necessary to introduce a smaller generation size such as 16, 32, and 64 bytes to improve the reliability and E2E delay, as well as to study the effect of reducing the generation size in an industrial setting.

Thus, the Raptor Q codes can be a good candidate for obtaining results within a strict range of requirements set by the URC use case. As a result, RLNC can be replaced with other common classes of rateless codes, such as Raptor Q, for reliable source coding, especially in an indoor factory deployment.

Data Availability

No data were used to support this study.

Conflicts of Interest

The authors declare that they have no conflicts of interest.

Authors' Contributions

All authors conceived and design the study. Athirah Mohd Ramly conducted the experiment, analyzed the data, and wrote the paper. All authors contributed to manuscript revisions. All authors approved the final version of the manuscript and agree to be held accountable for the content therein.

Acknowledgments

This work was supported in part by the Center for Research and Instrumentation (CRIM) and the Faculty of Engineering and Built Environment (FKAB), Universiti Kebangsaan Malaysia (UKM), and in part by the Malaysian Ministry of Education and Universiti Kebangsaan Malaysia Research Grant under Grant GUP-2021-023.

References

[1] Huawei, "5G ToB Service Experience Standard Whitepaper," 2021, https://carrier.huawei.com/~/media/CNBGV2/download/products/servies/5g-b2b-service-experience-standard-white-paper-en1.pdf.

[2] S. R. Pokhrel, J. Ding, J. Park, O. -S. Park, and J. Choi, "Towards enabling critical mMTC: a review of URLLC within mMTC," *IEEE Access*, vol. 8, pp. 131796–131813, 2020.

[3] D. Feng, C. She, K. Ying et al., "Toward ultrareliable low-latency communications: typical scenarios, possible solutions, and open issues," *IEEE Vehicular Technology Magazine*, vol. 14, no. 2, pp. 94–102, 2019.

[4] M. Luby, "LT codes," in *The 43rd Annual IEEE Symposium on Foundations of Computer Science, 2002. Proceedings*, pp. 271–280, Vancouver, BC, Canada, 2002.

[5] A. Shokrollahi, "Raptor codes," *IEEE Transactions on Information Theory*, vol. 52, no. 6, pp. 2551–2567, 2006.

[6] M. Luby, A. Shokrollahi, M. Watson, and T. Stockhammer, "Raptor forward error correction scheme for object delivery," *Internet Engineering Task Force (IETF), RFC 5053*, vol. 11, no. 3, pp. 82–89, 2007.

[7] S. Nie, S. Gu, J. Jiao, W. Xiang, and Q. Y. Zhang, "A novel systematic raptor network coding scheme for Mars-to-Earth relay communications," in *2016 IEEE Wireless Communications and Networking Conference*, pp. 1–6, Doha, Qatar, 2016.

[8] M. Shirvanimoghaddam, M. Dohler, and S. J. Johnson, "Massive multiple access based on superposition Raptor codes for cellular M2M communications," *IEEE Transactions on Wireless Communications*, vol. 16, no. 1, pp. 307–319, 2017.

[9] M. T. Gul, A. Ali, D. K. Singh et al., "Merge-and-forward: a cooperative multimedia transmissions protocol using RaptorQ code," *IET Communications*, vol. 10, no. 15, pp. 1884–1895, 2016.

[10] A. Shokrollahi and M. Luby, "Raptor codes," *Foundations and Trends in Communications and Information Theory*, vol. 6, no. 3-4, pp. 213–322, 2011.

[11] 3GPP, *UMTS; LTE; Multimedia Broadcast/Multicast Service (MBMS)*, Protocols and Codecs, 2015.

[12] M. Samokhina, K. Suwon, K. Moklyuk, S. Choi, K. Seoul, and J. He, "Raptor code-based video multicast over IEEE 802.11 WLAN," in *IEEE APWCS*, Citeseer, 2008.

[13] X. Chen, V. Subramanian, and D. J. Leith, "PHY modulation/rate control for fountain codes in 802.11a/g WLANs," *Physical Communications*, vol. 9, no. 9, pp. 135–144, 2013.

[14] J. Calabuig, J. Monserrat, D. Gozalvez, and D. Gomez-Barquero, "AL-FEC for streaming services in LTE E-MBMS," *EURASIP Journal on Wireless Communications and Networking*, vol. 2013, no. 1, pp. 1–12, 2013.

[15] N. Ma and M. Diao, "CoFi: Coding-assisted file distribution over a wireless LAN," *Symmetry*, vol. 11, no. 1, p. 71, 2019.

[16] J. Heide, M. V. Pedersen, F. H. P. Fitzek, and T. Larsen, "Network coding for mobile devices-systematic binary random rateless codes," in *2009 IEEE International Conference on Communications Workshops*, pp. 1–6, Dresden, Germany, 2009.

[17] Y. Li, S. Blostein, and W.-Y. Chan, "Systematic network coding for two hop lossy transmissions," *EURASIP Journal on Advances in Signal Processing*, vol. 2015, no. 1, 2015.

[18] S. Pandi, F. Gabriel, J. A. Cabrera, S. Wunderlich, M. Reisslein, and F. H. P. Fitzek, "PACE: redundancy engineering in RLNC

for low latency communication," *IEEE Access*, vol. 5, pp. 20477–20493, 2017.

[19] L. Wei and W. Chen, "Compute-and-forward network coding design over multi-source multi-relay channels," *IEEE Transactions on Wireless Communications*, vol. 11, no. 9, pp. 3348–3357, 2012.

[20] D. Malak, E. Ohad, M. Médard, and E. M. Yeh, "Throughput and delay analysis for coded ARQ," in *2019 International Symposium on Modeling and Optimization in Mobile, Ad Hoc, and Wireless Networks (WiOPT)*, pp. 1–8, Avignon, France, 2019.

[21] D. Malak, M. Medard, and E. M. Yeh, "Tiny codes for guaranteeable delay," *IEEE Journal on Selected Areas in Communications*, vol. 37, no. 4, pp. 809–825, 2019.

[22] M. Kim, K. Park, and W. W. Ro, "Benefits of using parallelized nonprogressive network coding," *Journal of Network and Computer Applications*, vol. 36, no. 1, pp. 293–305, 2013.

[23] S. Lee and W. W. Ro, "Accelerated network coding with dynamic stream decomposition on graphics processing unit," *The Computer Journal*, vol. 55, no. 1, pp. 21–34, 2012.

[24] H. Shojania, B. Li, and X. Wang, "Nuclei: GPU-accelerated many cores network coding," in *IEEE Infocom*, pp. 459–467, Rio de Janeiro, Brazil, 2009.

[25] S.-M. Choi, K. Lee, and J.-S. Park, "Fast parallel implementation for random network coding on embedded sensor nodes," *International Journal of Distributed Sensor Networks*, vol. 10, no. 2, Article ID 974836, 2014.

[26] K. Park, J.-S. Park, and W. W. Ro, "On improving parallelized network coding with dynamic partitioning," *IEEE Transactions on Parallel and Distributed Systems*, vol. 21, no. 11, pp. 1547–1560, 2010.

[27] H. Shin and J.-S. Park, "Energy efficient QoS-aware random network coding on smartphones," *Mobile Networks and Applications*, vol. 22, no. 5, pp. 880–893, 2017.

[28] H. Shin and J.-S. Park, "Reducing energy consumption of RNC based media streaming on smartphones via sampling," *Multimedia Tools and Applications*, vol. 78, no. 20, pp. 28461–28475, 2019.

[29] S. Wunderlich, J. A. Cabrera, F. H. P. Fitzek, and M. Reisslein, "Network coding in heterogeneous multicore IoT nodes with DAG scheduling of parallel matrix block operations," *IEEE Internet of Things Journal*, vol. 4, no. 4, pp. 917–933, 2017.

[30] R. Ahlswede, N. Cai, S.-Y. R. Li, and R. W. Yeung, "Network information flow," *IEEE Transactions on Information Theory*, vol. 46, no. 4, pp. 1204–1216, 2000.

[31] J. He, V. Tervo, X. Zhou et al., "A tutorial on lossy forwarding cooperative relaying," *IEEE Communications Surveys & Tutorials*, vol. 21, no. 1, pp. 66–87, 2019.

[32] M. El Soussi, A. Zaidi, and L. Vandendorpe, "Compute-and-forward on a multiaccess relay channel: Coding and symmetric-rate optimization," *IEEE Transactions on Wireless Communications*, vol. 13, no. 4, pp. 1932–1947, 2014.

[33] F. Gabriel, S. Wunderlich, S. Pandi, F. H. P. Fitzek, and M. Reisslein, "Caterpillar RLNC with feedback (CRLNC-FB): reducing delay in selective repeat ARQ through coding," *IEEE Access*, vol. 6, pp. 44787–44802, 2018.

[34] J. K. Sundararajan, D. Shah, M. Medard, and P. Sadeghi, "Feedback based online network coding," *IEEE Transactions on Information Theory*, vol. 63, no. 10, pp. 6628–6649, 2017.

[35] P. U. Tournoux, E. Lochin, J. Lacan, A. Bouabdallah, and V. Roca, "On-the-Fly erasure coding for real-time video applications," *IEEE Transactions on Multimedia*, vol. 13, no. 4, pp. 797–812, 2011.

[36] S. Wunderlich, F. Gabriel, S. Pandi, F. H. P. Fitzek, and M. Reisslein, "Caterpillar RLNC (CRLNC): a practical finite sliding window RLNC approach," *IEEE Access*, vol. 5, pp. 20183–20197, 2017.

[37] I. Chatzigeorgiou and A. Tassi, "Decoding delay performance of random linear network coding for broadcast," *IEEE Transactions on Vehicular Technology*, vol. 66, no. 8, pp. 7050–7060, 2017.

[38] A. Douik and S. Sorour, "Data dissemination using instantly decodable binary codes in fog-radio access networks," *IEEE Transactions on Communications*, vol. 66, no. 5, pp. 2052–2064, 2018.

[39] M. Nistor, D. E. Lucani, T. T. V. Vinhoza, R. A. Costa, and J. Barros, "On the delay distribution of random linear network coding," *IEEE Journal on Selected Areas in Communications*, vol. 29, no. 5, pp. 1084–1093, 2011.

[40] J. Qureshi, C. H. Foh, and J. Cai, "Online XOR packet coding: efficient single-hop wireless multicasting with low decoding delay," *Computer Communications*, vol. 39, pp. 65–77, 2014.

[41] H. Tang, Q. T. Sun, Z. Li, X. Yang, and K. Long, "Circular-shift linear network coding," *2017 IEEE International Symposium on Information Theory (ISIT)*, vol. 65, no. 1, pp. 65–80, 2019.

[42] D. E. Lucani, M. V. Pedersen, D. Ruano et al., "Fulcrum: flexible network coding for heterogeneous devices," *IEEE Access*, vol. 6, pp. 77890–77910, 2018.

[43] V. Nguyen, E. Tasdemir, G. T. Nguyen, D. E. Lucani, F. H. P. Fitzek, and M. Reisslein, "DSEP fulcrum: dynamic sparsity and expansion packets for fulcrum network coding," *IEEE Access*, vol. 8, pp. 78293–78314, 2020.

[44] M. Luby, L. Minder, and P. Aggarwal, *Performance of CodornicesRq software package*, International Computer Science Institute, 2019.

[45] A. M. Ramly, N. F. Abdullah, and R. Nordin, "Cross-layer design and performance analysis for ultra-reliable factory of the future based on 5G Mobile networks," *IEEE Access*, vol. 9, pp. 68161–68175, 2021.

[46] METIS II, *METIS II, V.1, Deliverable D2.1., "Performance Evaluation Framework"*, METIS II, 2016.

[47] GPP TS, *Service Requirements for next generation new services and markets*, ETSI, 2018.

[48] M. H. Alsharif, R. Nordin, M. M. Shakir, and A. Mohd Ramly, "Small cells integration with the macro-cell under LTE cellular networks and potential extension for 5G," *Journal of Electrical Engineering and Technology*, vol. 14, no. 6, pp. 2455–2465, 2019.

[49] K. Zhang, Q. Zhang, and J. Jiao, "Bounds on the reliability of RaptorQ codes in the finite-length regime," *IEEE Access*, vol. 5, pp. 24766–24774, 2017.

[50] A. H. Kelechi, M. H. Alsharif, A. M. Ramly, N. F. Abdullah, and R. Nordin, "The four-C framework for high capacity ultra-low latency in 5G networks: a review," *Energies*, vol. 12, no. 18, p. 3449, 2019.

[51] M. V. Pedersen, J. Heide, and F. Fitzek, "Kodo: an open and research oriented network coding library," *Lecture Notes in Computer Science*, vol. 6827, pp. 145–152, 2011.